Effect of Temperature and Microstructure on Hot Ductility Properties of a Boron Steel

A. Dimatteo, G. Lovicu, M. DeSanctis, R. Valentini

Dipartimento di Ingegneria Chimica, Chimica Industriale e Scienza dei Materiali; Università di Pisa; largo Lucio Lazzarino, 2 - 56126 Pisa (Italy) - a.dimatteo@diccism.unipi.it

ABSTRACT. *In recent years, the hot ductility properties of steel at slow strain rates has become important because of its relationship to the problem of transverse cracking observed during continuous casting (CC). These cracks are believed to form when the strand, usually cast in curved mould, is straightened in the temperature range between 700 and 1200°C.*

In this paper, the hot ductility properties of a boron microalloyed steel has been investigated by hot tensile tests carried out at the temperatures of 700-800-900-1000-1100-1200°C. Investigation have been performed by SEM on specimens longitudinal sections in order to analyse the relationship between microstructural features and crack path.

Results have shown that the microstructural features of the tested samples play a very important role in the formation and propagation of cracks and they influence the steel susceptibility to the transverse crack formation in CC steels.

INTRODUCTION

In the continuous casting steelmaking process during the straightening operation, the top surface of the slab is tensile tensioned at temperatures (700-1200°C) and strain rates (10^{-3} and 10^{-4} s^{-1}) at which most steels present poor ductility. In these conditions continuous cast products can suffer of transverse cracking. [1-3]

Hot ductility of low carbon steel is influenced by several factors, especially temperature, chemical composition, strain rate and thermal history. There are three critical temperature regions characterized by heavy reduction of ductility: the region close to the melting point, the region of austenite, the austenite-ferrite two phase region. [4]

Even though extensive work has been done to solve this problem, hot cracking still persists. A current trend in steel processing technology is to integrate the rolling process with the continuous casting process through “direct rolling” (rolling of hot slabs without reheating) or “hot charging” (charging of hot slabs into the reheating furnace). This does not allow for any tolerance of surface cracks, since there is no interruption between casting and subsequent hot rolling processes for inspection and scarfing. [5]

Evaluation of steel sensitivity to hot cracking is usually carried out by drawing hot ductility curves, showing the reduction of area of specimens fractured in tension as a

function of temperature. A typical hot-ductility curve distinctively shows an intermediate temperature region featuring a ductility trough where the embrittlement effect occurs with the highest evidence. [1-5]
Generally, the mechanisms of the hot ductility loss in steel have been attributed to the grain boundary, or the region adjacent to the grain boundary, which can be weaker than the grain interior.[5] This leads to strain concentrations at or near the grain boundary and, consequently, grain boundary decohesion.
An important factor, which affects the steel slab surface cracking in the continuously casting process, is hot ductility of steel in the temperature range of the $\gamma \rightarrow \alpha$ transformation at a low strain rate. [6] The embrittlement of low carbon steels in this two phase region is principally caused by thin film formation of proeutectoid ferrite along the austenite grain boundaries. The localised strain in the proeutectoid ferrite film results in crack formation and microvoid coalescence both in proeutectoid ferrite and at the γ - α interface. The hot ductility loss in this temperature region can be increased by MnS or AlN inclusion precipitation and precipitation of microalloying elements (Nb, V, Ti) particles. These precipitates on austenite grain boundaries are initial points for microvoid formation. [7]
In this paper, a boron microalloyed steel has been used to investigate its hot ductility properties. Analyses of possible microstructural damage during plastic straining of the steels were carried out by SEM in combination with X-ray Energy Dispersive Spectrometer (EDS) microanalysis.

EXPERIMENTAL PROCEDURE AND RESULTS

A high performance steel (35KB2, 1075MPa of Ultimate strength and 990MPa of Yield strength) has been reproduced in laboratory. A heat of about 15 kg has been prepared by induction melting in argon atmosphere. It was thermally treated to homogenize the structure and samples for Continuous Cooling Transformation (CCT) diagram determination and hot tensile tests were machined. The chemical composition of the investigated steel is given in Table 1.

Table 1: chemical composition of the tested steel

C	Mn	Si	P	S	Cr	Mo	Al	V	Nb	Ti	B
0.35	1.19	0.24	0.024	0.018	0.2	0.02	0.026	0.005	0.003	0.054	0.0027

a. CCT Diagrams

A Gleeble-3800 thermomechanical simulator was used to determine the experimental transformation diagrams during continuous cooling. A thermal cycle was specifically designed: the specimens were austenitized at 1573 K with a heating rate of 2.5 K/s. This temperature was maintained for 60 seconds. Finally, the specimens were cooled to room temperature with constant cooling rates of 0.1, 0.35, 0.6, 1, 1.5, and 2 K/s.

Transformation temperature and times were determined by the obtained dilatation curves and by using microstructural analysis and hardness test on the investigated samples.
Microstructural analysis show that the microstructure of tested steel is composed of ferrite and pearlite for the lower cooling rates (0.1-0.35°C/s). For the intermediate cooling rates (0.6-1°C/s) it is composed by ferrite, pearlite and bainite. Finally, for the higher cooling rates (1.5-2°C/s) it is composed by very few pearlite and bainite.

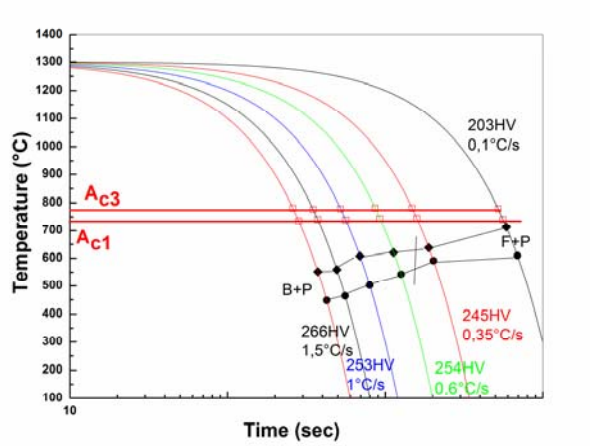

Figure 1. Experimental CCT for the tested steel.

The CCT diagram for the tested steel is shown in Fig.1. Cooling rates and Vickers hardness are indicated close to each cooling curve. Also the A_{c3} and A_{c1} temperatures are reported. The transformation behaviour of austenite during cooling at several different rates can be seen from the CCT diagrams of the tested steel.

b. Hot ductility tests

Hot ductility was investigated by hot tensile tests performed using a Gleeble 3800 machine. The thermomechanical cycle used to simulate the straightening operation is as follows: heating to 1420°C at a rate of 10°C/s and holding at this temperature for 20s, then cooling to the test temperatures (700-800-900-1000-1100-1200°C) at three different cooling rates: 0.5-1-2°C/s and, finally, test and cooling in air to room temperature.
Samples were sectioned longitudinally with respect to the rolling direction and metallographic analysis has been performed on the region close to the surface fracture. Deformed microstructures were characterized by optical microscopy and scanning electron microscopy equipped with EDX technique.
Both cooling rates and strain rate (10^{-3} s^{-1}) were close to the ones experienced by the billet surface during the straightening operation. Hot ductility was quantified by the reduction in area (%RA) of the tested samples as a function of temperature (see Fig. 2).

For all the tested cooling rates, there was no minimum of ductility. Moreover the ductility is over 60% for all the tested temperature apart for the lower tested temperature of 700°C for which the RA is lower than 50%.

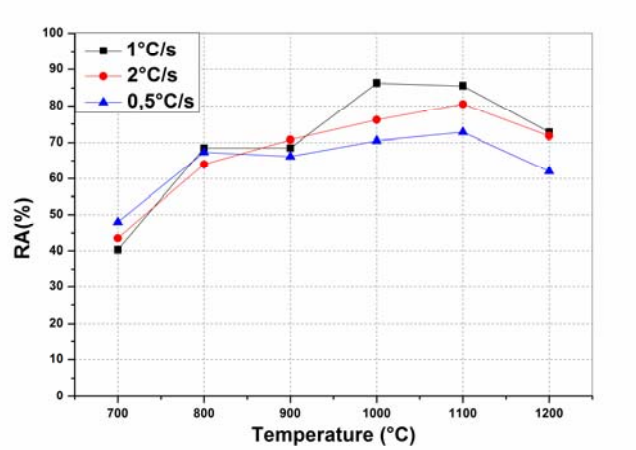

Figure 2. Hot ductility curves

According to several authors (see for example [8]) the temperature range in which the RA is less than or equal to 60% is a crack sensitive range for continuous casting, which is called the hot brittle range. In terms of this rule, in the present steels, the hot brittle range is for temperatures lower than 800°C.
Examples of the obtained stress–elongation curves are shown in Fig. 3. For temperature range 1000–1200 °C, there were fluctuations in the flow curves for all examined steels. Such fluctuations are evidence of dynamic recrystallization which is usually characterized either by a sudden drop or by oscillation in the flow curve [8].
At 700°C the high strain hardening indicates the absence of recrystallization.

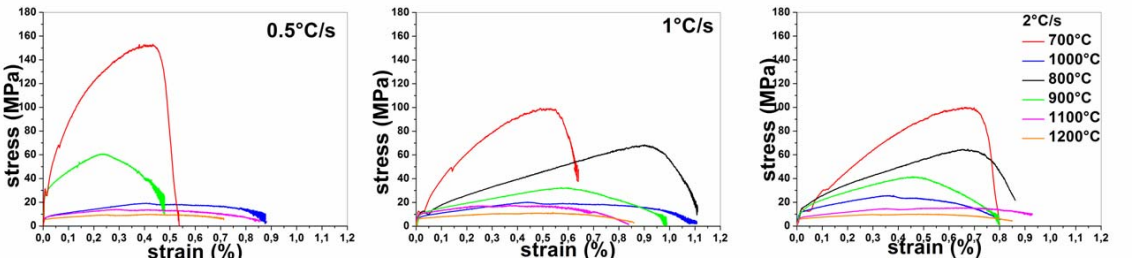

Figure 3. Stress strain curves recorded at the different tested temperatures for all the three tested temperatures.

c. Microstructural investigation of crack path

The microstructures longitudinal section of deformed samples were characterized using optical and electron microscopy and were taken from the neck region. Microstructures after deformation are shown in Fig. 4 for the lower and highest tested temperatures.

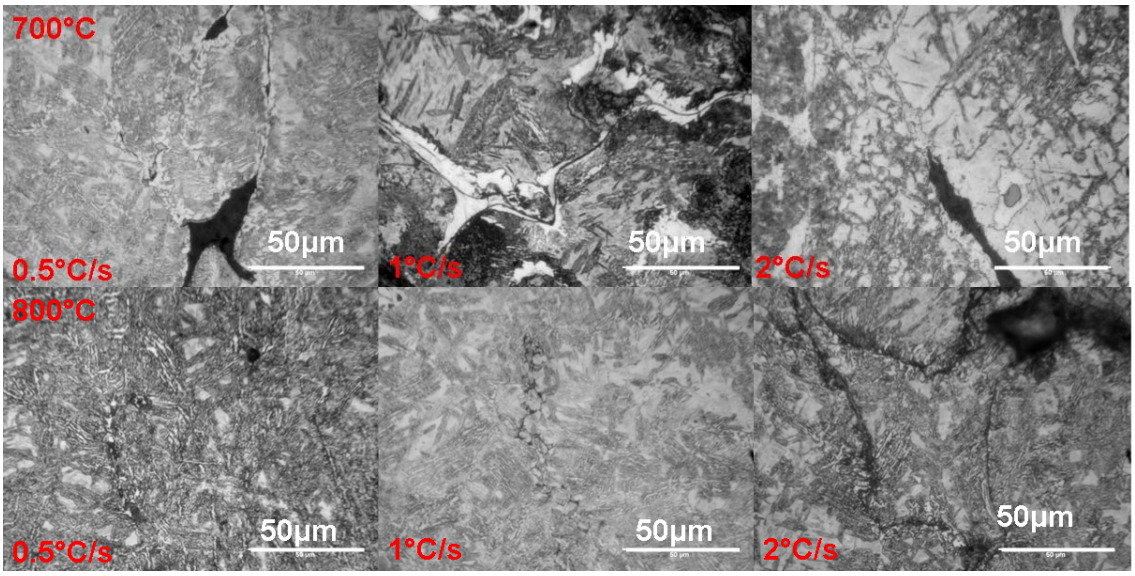

Figure 4. Microstructures of samples tested at 700 and 1200 °C

As visible in Fig.4, for the lowest testing temperature (700°C), the microstructure of the samples consisted of ferrite on the prior austenite grain boundaries and ferritic bainite. For all the other conditions the microstructure is totally acicular.

From the CCT diagram in Fig.1, it is readable that 700°C is slight over the transformation temperature for all the investigated cooling rates. The ferrite formation at 700°C is due both to the deformation that increase the transformation kinetic both to the isothermal transformation due to the maintenance at 700°C for the time of the hot tensile tests. It is well visible that, for the lowest testing temperature (700°C), cracks are present within ferritic grain size. Ferrite is softer than austenite at elevated temperatures, due to a higher dynamic recovery rate. This allows strain to concentrate in the ferrite film, encouraging voiding around precipitates and/or inclusions situated at the boundaries. These voids link up to give failure by microvoid coalescence. [8]

The microstructure for the higher cooling rates (1-2°C/s) consists of Widmanstätten ferrite on the prior austenite grain boundaries and bainite with acicular ferrite. The zig-zag shape cracks with inclusions inside or crack paths along the prior austenite grain boundaries can be observed. The precipitate particles have two major roles; they can delay the onset of recrystallisation, and they can reduce the strain required for fracture by a number of possible mechanisms: precipitate free zones are often observed adjacent to austenite grain boundaries, and this may lead to strain concentration at the grain boundary; the particles (or groups of particles) at the grain boundaries may act as crack initiation sites; or general matrix precipitation can lead to an increase in strength, and an overall reduction in ductility. The proposed mechanism consists of nucleation of microvoids at numerous sites of precipitates followed by cracking between ferrite or bainite laths and coalescence of microvoids to microcracks. Then the microcracks were joined together for a final crack crossing the prior austenite grain boundaries or on a zig-zag path through large ferrite grains and bainite packets.

The inclusion have been known to be detrimental to the mechanical properties of steel since they act as nucleation sites for microvoids and cracks. The most frequent inclusions in steels are sulphides. [10]
In the Fig.5, examples of MnS and Al_2O_3 inclusions can be seen. Void around the inclusions is present, and in their neighbourhood there is a bigger microcrack on the grain boundary.

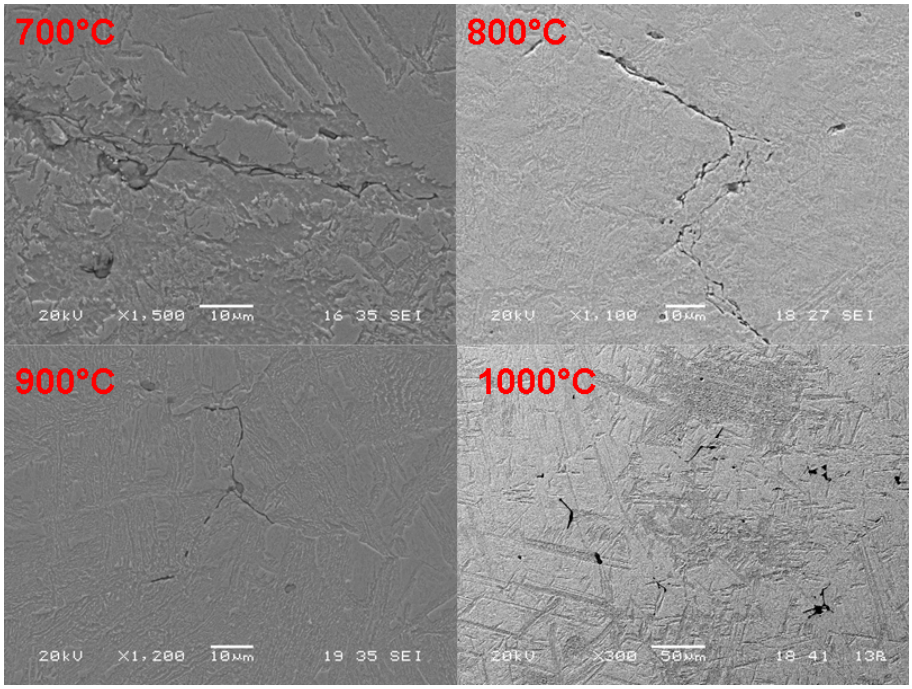

Figure 5: Examples of crack paths for specimen cooled at 2°C/s.

In particular, at 700°C microcracks nucleated at the carbide particles in the ferrite phase at prior austenite grain boundaries. At 800 and 900°C, microcracks nucleated at the carbide particles at prior austenite grain boundaries. Carbide particles in lath boundaries can cause kinks and branching of the crack. At 1000°C, the specimen had fractured through grain boundary decohesion. Cracks initiated at grain boundary triple junctions and propagated along the boundaries, leading to complete separation of grains.

Discussion

The microstructure in the sample neck depends on the test temperature and cooling rate before the test temperature. One of the factors, which has a strong influence on the microstructure is the temperature of deformation. The microstructure after deformation depends on what kind of microstructure were present before deformation. In the lower temperature of deformation (700°C) there were austenite and ferrite in the structure. Above this temperature there was only austenite in the sample structure before deformation.

Through the fracture features observed by SEM and OM, it is possible to relate the fracture behaviour of the present steel with different mechanisms, depending on the test temperature and thermal cycle applied to the samples.
Generally speaking, examination of microstructures quenched immediately after fracture revealed that the failure was associated with grain boundary microcracks (Fig.5). Linkage of microcracks in some regions resulted in formation of macrocracks and grain boundary cavities.
At low temperatures, the mechanism responsible for reducing the ductility of the steel is the formation of a thin ferrite layer surrounding the previous austenite grains, Fig.4. The thin films of ferrite which surround the austenite grains, allows strain concentration to occur and produces micro-voids around the precipitates particles situated at the boundaries (Fig.5), with the voids eventually linking up to give intergranular fracture [9].
Intergranular failure of samples in the austenite temperature region can be explained by the influence of different mechanisms that relate with the presence of inclusions. The observed fine precipitation at the austenite grain boundaries are particularly effective in preventing grain boundary mobility and reducing ductility, leading to the observed intergranular fracture and widening of the trough [10].
Examination of the microstructure near the fracture region (Fig. 5) explicitly shows that grain boundary separation was a result of void formation and coalescence at grain boundaries, mostly at grain boundary triple junctions. It was also noticed that the void formation process was assisted by grain boundary MnS and Al_2O_3 particles. The EDS spectra collected during qualitative analyses of the precipitates showed that the particles affecting grain-boundary cohesion were rich in microalloying elements already recognized in other literature studies.
The excellent ductility at the temperature range 1000–1200 °C is attributed to dynamic recrystallization. Mintz et al. [4] believed that recrystallization and movement of grain boundaries prevent voids linking up giving high RA values. In fact, during recrystallization, grain boundaries migrate and microvoids initially formed at grain boundaries are isolated from the boundaries. Consequently, the coalescence of microvoids at grain boundaries is prevented and grain boundary decohesion is retarded. However, some improvement of ductility may be also attributed to either reducing the degree of precipitation or coarsening the existing precipitates.
The stress-strain curves in Fig. 3 show that the higher RA values correspond to the temperatures for the onset of dynamic recrystallisation.
From these results, it can be concluded that the occurrence of dynamic recrystallization at the straightening stage is the reason for the good hot ductility in the tested steel.

Conclusions

The processes that are responsible for the ductility loss during hot deformation in a boron microalloyed steel are explored. Two major mechanisms, namely the formation

of Nb(CN) precipitates and the formation of ferrite films and ferrite islands at lower temperatures were identified.
The occurrence of dynamic recrystallization in the range between 1000 and 1200 °C had a substantial contribution to the high ductility observed in this range of temperatures.

References

1. Lis, A., Lis, J., Kolan, C., Knapiński, M., Effect of strain rate on hot ductility of C-Mn-B steel (2010) Journal of Achievements in Materials and Manufacturing Engineering 41(1-2), 26-33.
2. N. Wolañska, N., A.K. Lis, A.K., J. Lis, J., Investigation of C-Mn-B steel after hot deformation (2007) Archives of Materials Science and Engineering 28(2), 119-125.
3. Vedani, M., Ripamonti, D., Mannucci, A., Dellasega, D.: HOT DUCTILITY OF MICROALLOYED STEELS (2008) La Metallurgia Italiana May, 19-24.
4. Mintz, B., Abushosha, R., influence of vanadium on hot ductility of steel (1993) IronMaking and SteelMaking 20(6), 445-452.
5. Zarandi, F., Yue, S., Failure Mode Analysis and a Mechanism for Hot-Ductility Improvement in the Nb-Microalloyed Steel (2004) Metallurgical and Materials Transactions A 35A, 3823-3832
6. Calvo, J., Rezaeian, A., Cabrera, J.M., Yue, S., Effect of the thermal cycle on the hot ductility and fracture mechanisms of a C–Mn steel, (2007) Engineering Failure Analysis 14, 374–383
7. Vedani,M., Dellasega, D., Mannucci, A., Characterization of Grain-boundary Precipitates after Hot-ductility Tests of Microalloyed Steels (2009) ISIJ International 49(3), 446–452.
8. Lopez-Chipres, E., Mejıa, I., Maldonado, C., Bedolla-Jacuinde, A., Cabrera, J.M., Hot ductility behavior of boron microalloyed steels (2007) Materials Science and Engineering A 460–461, 464–470.
9. Maehara, Y, Yasumoto, K., Tomono, H., Nagamichi, T., Ohmori, Y. Surface Cracking Mechanism of Continuously Cast Low Carbon Low Alloy Steel Slabs (1990) Mat. Sci. and Technol. 6, 793-806.
10. Kim, T.K. , Jang, J., Ryu, W.S., Hong, J.H., Mitchell, A. Influence of Precipitation and Grain Size on the Hot Ductility of Alloy C-276 ESR Ingots (2001) High Temperature Materials and Processes 20(2), 143-154.